

Benchmarking of Collision Operators with Momentum Source Corrections

H. Maaßberg*, and C.D. Beidler

Max-Planck-Institut für Plasmaphysik,

EURATOM Association, D-17491 Greifswald, Germany

(Dated: March 22, 2010)

Abstract

Several linearised collision operator models with parallel momentum conservation enforced by source functions are benchmarked against the correct collision operator based on Rosenbluth potentials. The model operators without energy diffusion allow for an analytic solution of a *generalised* Spitzer problem. For the other operators under investigation, an integro-differential equation is solved. The benchmarking is performed both for the parallel conductivity with the ions assumed at rest and for the bootstrap current, where ion and electron flows are collisionally coupled. Accuracy of the results obtained with the operators varies from rather poor in the case of the simplest mono-energetic model to quite satisfactory for the models employing an energy-weighted parallel momentum source function.

* E-mail: maass@ipp.mpg.de

I. INTRODUCTION

Momentum conservation in the collision operator is essential for evaluating the parallel flows in a plasma, e.g. the parallel electric conductivity and the bootstrap current in toroidal fusion devices. In general, the collision operator is linearised with respect to a small deviation, δf , from the Maxwellian, F_M . Then, the operator splits into a diffusion term for δf with the background Maxwellians in the Rosenbluth potentials [1], i.e. in the diffusion coefficients, and into an integral part with δf in the *1st-order* Rosenbluth potentials. An example is the classical Spitzer problem [2] for the electric conductivity which is obtained from the solution of this integro-differential equation.

Recently, parallel momentum correction techniques for stellarators have been developed [3–6], which make use of the three mono-energetic transport coefficients (for benchmarking results see [7]) traditionally used in the stellarator neoclassical theory. These coefficients are obtained from the solution of the local and mono-energetic drift-kinetic equation with the Lorentz form of the pitch-angle collision term, which does not conserve parallel momentum in like-particle collisions. Since Legendre polynomials in the pitch, $p = v_{\parallel}/v$, are eigenfunctions of the collision operator [1], only the first ($l = 1$) Legendre harmonic is needed for the momentum correction. The Vlasov operator in the drift-kinetic equation, however, leads to coupling in the Legendre harmonics. The parallel viscosity is linked to the pressure anisotropy, i.e. to the second Legendre harmonic. By solving the mono-energetic drift-kinetic equation, the parallel viscosity can be found from the mono-energetic parallel momentum balance [6] using the parallel conductivity coefficient. This leads to a *generalised* Spitzer problem for the energy dependence, i.e. a coupled system of integro-differential equations for all particle species under consideration, but with regard only to the first Legendre harmonic. Alternately, the correction may be formulated in terms of a system of linear equations coupling various energy moments of the parallel flow velocities of all plasma species. This moment equation approach [3–6] can be obtained by a Sonine (generalised Laguerre) polynomial expansion with respect to energy of the *generalised* Spitzer problem.

For linearised (gyroaveraged) collision operators (finite gyroradius effects, however, are not important in this context) in Monte Carlo simulation techniques, the integral contributions from the 1st-order Rosenbluth potentials are replaced by a parallel momentum (and energy) source function in Refs. [8, 9] with the source strength determined from the parallel momentum (and energy) balance of this simplified like-particle collision term. The main argument for this approximation

(even justified with the identical formulation in [8, 9]) is that the solution of the kinetic equation for δf is not sensitive to the details of δf in the 1st-order integral contributions [9]. In Monte Carlo techniques, this approach has the advantage that the energy dependence of the parallel momentum (and energy) source function is fixed whereas the integral contributions from the 1st-order Rosenbluth potentials depend on the energy dependence of δf itself (requiring an additional energy grid). Only the total parallel momentum (and energy) source strength can be easily estimated from the like-particle collision operator [10] in the Monte Carlo techniques. With this simplification, however, the different plasma species are coupled only by the diffusive part of the collision operator, e.g. the parallel momentum transfer from ions to electrons is not correctly included [8, 9]. As the parallel electron flow is strongly coupled to the parallel ion flow, here the 1st-order ion integral contributions on the electron δf cannot be ignored. This problem is removed if the electron-ion collision operator with only pitch-angle scattering included is formulated in the ion frame [11–13]. In this paper, a more precise treatment, which is a generalisation of the electron Ohkawa current contribution for neutral beam current drive [14, 15], is applied for the benchmarking of these simplified collision operators with respect to the bootstrap current.

Several simplified collision operators with like-particle momentum conservation are benchmarked in this paper against the correct linearised operator for the first Legendre harmonic with the 1st-order Rosenbluth potentials for all plasma species included [6]. The most simplified case is a strict mono-energetic operator with only pitch-angle collisions and momentum correction for each energy separately, i.e. the like-particle pitch-angle collisions are omitted in the correction technique; this model operator represents a worst case for reference. Since momentum conservation is strictly defined only in an integrated form, collision operators without energy diffusion but with different energy-weighted parallel momentum source terms are analysed. The operator with the weighting function introduced in Refs. [16, 17] is also included in this benchmarking. This form of the pitch-angle collision operator was applied in Ref. [18] in Monte Carlo simulations of tokamak neoclassical transport, and in particular in [12] for estimating the bootstrap current. The other model operators include energy diffusion [8, 9, 13, 19] and differ only in the energy weighting function of the parallel momentum source. The benchmark is performed only for a pure plasma with a single ion species as plasmas with multiple ions species require a more complex treatment [20] in particular for the bootstrap current.

The paper is organised as follows. In Sec. II, the *generalised* Spitzer equation of Ref. [6] is briefly described which is the basis of the benchmarking of the simplified collision operators both

for the electric conductivity and for the bootstrap current. The correct collision operator as well as the parallel momentum sources needed for the simplified like-particle operators is summarised. Finally, the Green’s function describing the impact of the parallel ion flow on the electron one is derived. Section III gives examples for the benchmarking of the collision operators under investigation at finite collisionalities for the W7-X “standard” configuration [21] at half the plasma radius. All the calculations are based on a precalculated database of mono-energetic transport coefficients from the DKES code [22, 23]. Finally, a summary and conclusions are given in Sec. IV.

II. THE MODELS IN THE BENCHMARKING

First, the basic equation for the benchmarking of this paper, the *generalised* Spitzer equation, is introduced and briefly discussed. This equation is independent of details of the collision operators with parallel momentum conservation which are described later.

A. Generalised Spitzer equation

The deviation of the distribution function, δf , from the Maxwellian, F_M^α , is split in two portions, $f_1^\alpha + f_2^\alpha$ and $g_1^\alpha + g_2^\alpha$, for each particle species α . Here, the first portion is driven by the perpendicular thermodynamic forces A_1^α and A_2^α and the second one by the parallel force, A_3^α ,

$$A_1^\alpha = \frac{n'_\alpha}{n_\alpha} - \frac{q_\alpha E_r}{T_\alpha} - \frac{3}{2} \frac{T'_\alpha}{T_\alpha}, \quad A_2^\alpha = \frac{T'_\alpha}{T_\alpha} \quad \text{and} \quad A_3^\alpha = \frac{q_\alpha}{T_\alpha} \frac{\langle \mathbf{E} \cdot \mathbf{B} \rangle}{\langle B^2 \rangle} B_0,$$

where the prime represents the radial derivative, E_r the radial electric field, and $\langle \dots \rangle$ the flux-surface average. f_1^α and g_1^α are the solutions of the *local* and *mono-energetic* drift-kinetic equation (DKE) without momentum conservation, i.e. with the Lorentz form of the pitch-angle collision term, calculated e.g. by the DKES code [22, 23]. Then, f_2^α and g_2^α represent the result of the “error” in the parallel momentum conservation with respect to f_1^α and g_1^α . In the momentum correction techniques [3–6], only the first Legendre term of the flux-surface-averaged corrections is estimated based on the *mono-energetic* transport coefficients for the bootstrap current and the parallel conductivity (both are flux-surface-averaged moments of the Legendre term of degree $l = 1$). In Monte Carlo simulations, however, the collision operator models with like-particle momentum conservation act in full phase space. As described in detail in Ref. [6], the *generalised*

Spitzer equation for both the bootstrap current and the parallel conductivity component of \mathcal{K}^α may be expressed

$$C_{l=1}^\alpha(\mathcal{K}^\alpha) - \frac{f_t^{\text{eff}}}{f_c^{\text{eff}}} \nu^\alpha \mathcal{K}^\alpha = -\frac{1}{f_c^{\text{eff}}} \nu^\alpha \mathcal{K}_1^\alpha. \quad (1)$$

$C_{l=1}^\alpha$ is the first Legendre harmonic of any parallel-momentum-conserving collision operator under investigation. Here, $\mathcal{K}^\alpha = \mathcal{K}_1^\alpha + \mathcal{K}_2^\alpha$ and $\mathcal{K}_1^\alpha = (\Gamma_{31}^\alpha, \Gamma_{33}^\alpha)$ are the mono-energetic flows without momentum conservation with respect to the perpendicular thermodynamic forces (bootstrap current contribution Γ_{31}^α) and to the parallel force (Γ_{33}^α). Both the thermodynamic forces and the Maxwellian are dropped for the treatment of the (traditional) mono-energetic transport coefficients by defining $f_1^\alpha = \hat{f}_1^\alpha (A_1^\alpha + x^2 A_2^\alpha) F_M^\alpha$ and $g_1^\alpha = \hat{g}_1^\alpha A_3^\alpha F_M^\alpha$ where $x = x_\alpha = v/v_{th}^\alpha$. With the moments $[A] = \int_{-1}^1 \langle A \rangle dp/2$, the bootstrap current coefficient is defined by $D_{31}^\alpha = -v[bp\hat{f}_1^\alpha]$ and the electric conductivity coefficient by $D_{33}^\alpha = -v[bp\hat{g}_1^\alpha]$ where $b = B/B_0$ and $p = v_{||}/v$. Then, the mono-energetic flows $\mathcal{K}_1^\alpha = (\Gamma_{31}^\alpha, \Gamma_{33}^\alpha)$ may be expressed in the form

$$\Gamma_{31}^\alpha = -\frac{D_{31}^\alpha}{v} (A_1^\alpha + x^2 A_2^\alpha) F_M^\alpha \quad \text{and} \quad \Gamma_{33}^\alpha = -\frac{D_{33}^\alpha}{v} A_3^\alpha F_M^\alpha.$$

Parallel momentum correction is responsible for \mathcal{K}_2^α . For arbitrary collisionalities, $f_t^{\text{eff}}(x)$ is the effective trapped particle fraction in eq. (1) defined by using the mono-energetic conductivity coefficient D_{33}^α normalised to the Pfirsch-Schlüter value (at high collision frequencies ν^α)

$$f_t^{\text{eff}} = 1 - f_c^{\text{eff}} = 1 - D_{33}^\alpha \left(\frac{\nu^\alpha R}{vt} \right) \frac{3\nu^\alpha}{v^2 \langle b^2 \rangle} \quad (2)$$

with the mono-energetic ‘‘collisionality’’, $\nu^\alpha R/vt$ (R is the major radius and t the rotational transform). This definition guarantees the limits $f_t^{\text{eff}}(x \rightarrow 0) = 0$ (collisional) and $f_t^{\text{eff}}(x \rightarrow \infty) = f_t$ (collisionless) where f_t is the (geometrical) trapped particle fraction. The second term on the l.h.s. of eq. (1) represents the parallel viscosity (momentum sink by friction between the passing and trapped particles) and is formulated using the mono-energetic parallel momentum balance. $\nu^\alpha(x)$ is the collision frequency of species α . For the parallel conductivity, the r.h.s. reduces to $-v \langle b^2 \rangle A_3^\alpha F_M^\alpha/3$, i.e. the classical (collisional) Spitzer problem [2] apart from a constant factor is recovered for $f_t^{\text{eff}} \equiv 0$. Consequently, a slightly different form of Γ_{33}^α is used leading to the identical definition of the *classical* Spitzer problem for the benchmarking of the collision operators with respect to the parallel conductivity in Sec.III A.

B. Parallel momentum conserving collision operators

Different momentum conserving collision operators are included in this benchmarking which can be written in the form

$$C_{l=1}^\alpha(\mathcal{K}^\alpha) = C_v^\alpha(\mathcal{K}^\alpha) - \nu^\alpha \mathcal{K}^\alpha + \mathcal{P}^\alpha. \quad (3)$$

For the model operators with only pitch-angle scattering, $C_v^\alpha = 0$ is assumed. Otherwise, C_v^α describes the velocity diffusion with the diffusion coefficients defined from the Rosenbluth potentials with all Maxwellians, F_M^β , of species β .

$$C_v^\alpha(\mathcal{K}^\alpha) = \nu_o^\alpha \frac{1}{x^2} \frac{d}{dx} \left(a_1^\alpha \mathcal{K}^\alpha + \frac{1}{2} a_2^\alpha \frac{d}{dx} \mathcal{K}^\alpha \right) \quad (4)$$

with $x \equiv x_\alpha = v/v_{th}^\alpha$, $\nu_o^\alpha = n_\alpha (Z_\alpha e^2 / \varepsilon_0 m_\alpha)^2 \ln \Lambda / 4\pi (v_{th}^\alpha)^3$. The diffusion coefficients are given by

$$a_1^\alpha = \sum_\beta \frac{n_\beta Z_\beta^2 m_\alpha}{n_\alpha Z_\alpha^2 m_\beta} \eta(x_\beta), \quad a_2^\alpha = \sum_\beta \frac{n_\beta Z_\beta^2 v_{th}^\beta}{n_\alpha Z_\alpha^2 v_{th}^\alpha} \frac{\eta(x_\beta)}{x_\beta}, \quad \frac{\nu^\alpha}{\nu_o^\alpha} = \sum_\beta \frac{n_\beta Z_\beta^2 \widehat{\eta}(x_\beta)}{n_\alpha Z_\alpha^2 x_\alpha^3}$$

where $x_\beta = v/v_{th}^\beta$, $\eta(x) = \text{erf}(x) - \frac{2}{\sqrt{\pi}} x e^{-x^2}$ and $\widehat{\eta}(x) = \text{erf}(x) - \frac{\eta(x)}{2x^2}$. For a pure electron-ion plasma (with $Z_i = 1$ for simplicity), these coefficients are in leading order in $\sqrt{m_e/m_i}$

$$a_1^e = a_1^i = \eta(x), \quad a_2^e = a_2^i = \frac{\eta(x)}{x}, \quad \frac{\nu^i}{\nu_o^i} = \frac{1}{x^3} \widehat{\eta}(x), \quad \frac{\nu^e}{\nu_o^e} = \frac{1}{x^3} (1 + \widehat{\eta}(x)),$$

i.e. only the electron pitch-angle term is affected by the ions. In eq. (3), $-\nu^\alpha \mathcal{K}^\alpha$ is the first Legendre term of the pitch-angle collision operator, and \mathcal{P}^α is (the first Legendre term of) the momentum source function being responsible for parallel momentum conservation.

Correct collision operator

In eq. (3), the $l = 1$ integral contribution from the 1st-order Rosenbluth potentials for all species β is defined by (see [6])

$$\mathcal{P}^\alpha = \nu_o^\alpha e^{-x_\alpha^2} \sum_\beta \frac{n_\beta Z_\beta^2}{n_\alpha Z_\alpha^2} I^{\alpha\beta}(\mathcal{K}_2^\beta) \quad (5)$$

with

$$\begin{aligned} x_\alpha^2 I^{\alpha\beta}(\mathcal{K}^\beta) &= \frac{4}{\sqrt{\pi}} \frac{m_\alpha}{m_\beta} \frac{v_{th}^\alpha}{v_{th}^\beta} x_\beta^2 \mathcal{K}^\beta(x_\beta) - \frac{8}{3\sqrt{\pi}} \left(2 \frac{m_\alpha}{m_\beta} - 1 \right) \frac{v_{th}^\beta}{v_{th}^\alpha} \int_0^{x_\beta} (x'_\beta)^3 \mathcal{K}^\beta(x'_\beta) dx'_\beta \\ &+ \frac{16}{5\sqrt{\pi}} \left(\frac{v_{th}^\beta}{v_{th}^\alpha} \right)^3 \int_0^{x_\beta} (x'_\beta)^5 \mathcal{K}^\beta(x'_\beta) dx'_\beta + \frac{8}{3\sqrt{\pi}} \left(\frac{m_\alpha}{m_\beta} - 2 + \frac{6}{5} x^2 \right) x x_\beta^2 \int_{x_\beta}^\infty \mathcal{K}^\beta(x'_\beta) dx'_\beta. \end{aligned}$$

The operator of eq. (3) in this form conserves both the parallel momentum in like-particle collisions and the total parallel momentum for all plasma species. Contrary to the simplified collision operators, no special treatment of the momentum transfer from ions to electrons is required. For Monte Carlo techniques, however, this operator has the disadvantage that the evaluation of \mathcal{P}^α requires an additional x -grid which might lead to reduced statistical accuracy. For the solution of the *generalised* Spitzer equation (1), this operator is the reference case in the benchmarking.

Strict mono-energetic collision operator

The simplest form of a parallel momentum conserving collision operator is obtained by omitting the energy diffusion, i.e. $C_v^\alpha(\mathcal{K}^\alpha) = 0$, in eq. (3). The parallel momentum source function required for compensating the violation of the momentum conservation in like-particle collisions at each x is given by

$$\mathcal{P}^\alpha = \nu_0^\alpha \frac{\hat{\eta}(x)}{x^3} \mathcal{K}^\alpha.$$

For this model operator, the like-particle pitch-angle collision term in $C_{l=1}^\alpha$ in eq. (1) disappears and, consequently, the ion momentum correction is based only on the parallel viscosity. The *generalised* Spitzer equation (1) is solved analytically leading to

$$\mathcal{K}^i = \frac{1}{f_t^{\text{eff}}(x)} \mathcal{K}_1^i \quad \text{and} \quad \mathcal{K}^e = \frac{1 + \hat{\eta}(x)}{1 + f_t^{\text{eff}}(x)\hat{\eta}(x)} \mathcal{K}_1^e.$$

The like-particle collision frequency scales with $1/x^2$ ($\hat{\eta}(x) \propto x$ for $x \ll 1$) which can result in a large parallel momentum source function \mathcal{P}^α at small velocities depending on $\mathcal{K}^\alpha(x)$. This behaviour leads to a non-physical problem in the mono-energetic parallel momentum balance for the ions ($f_t^{\text{eff}}(x \rightarrow 0) \rightarrow 0$, i.e. the parallel viscosity vanishes) since a momentum source (e.g. the radial thermodynamic forces driving the parallel ion flow) cannot be balanced only by collisions.

Simplified collision operators with energy diffusion omitted

The integrated parallel momentum source strength must balance the integrated ‘‘error’’ in the like-particle collision operator of eq. (3) with $C_v^\alpha = 0$ assumed.

$$\int_0^\infty x^3 \mathcal{P}^\alpha dx = \nu_0^\alpha \int_0^\infty \hat{\eta}(x) \mathcal{K}^\alpha dx.$$

The parallel momentum source function should be proportional to the Maxwellian, $F_M^\alpha(x)$, but there is a freedom in the definition of $\mathcal{P}^\alpha(x)$ with respect to an arbitrary energy-dependent weighting function, $w(x)$,

$$\mathcal{P}^\alpha(x) = \nu_0^\alpha x w(x) F_M^\alpha(x) \frac{\int_0^\infty \hat{\eta}(x) \mathcal{K}^\alpha dx}{\int_0^\infty w(x) x^4 F_M^\alpha(x) dx}.$$

With $\mathcal{K}^\alpha = \mathcal{K}_1^\alpha + f_c^{\text{eff}} \mathcal{P}^\alpha / \nu^\alpha$ from eqs. (1) and (3), the analytic solution for \mathcal{P}^α (and for \mathcal{K}^α) is directly obtained

$$\mathcal{P}^\alpha = \nu_0^\alpha x w(x) F_M^\alpha \int_0^\infty \hat{\eta} \mathcal{K}_1^\alpha dx \cdot \left(\int_0^\infty \left(1 - f_c^{\text{eff}} \frac{\hat{\eta}}{\delta_{\alpha e} + \hat{\eta}} \right) w(x) x^4 F_M^\alpha dx \right)^{-1} \quad (6)$$

with $\delta_{ie} = 0$ and $\delta_{ee} = 1$. As is also the case for the strict mono-energetic model operator, the very small parallel viscosity at high collisionalities ($f_c^{\text{eff}} \rightarrow 1$) can lead to a problem for the ion parallel flow since the denominator in eq. (6) becomes very small. For collision operators with the C_v^α term taken into account, however, this problem at high collisionalities does not appear.

Three weighting functions $w(x)$ are considered in this benchmarking:

$$w_1 = 1; \quad w_2 = \frac{\eta(x)}{x^3} \quad \text{and} \quad w_3 = \frac{\hat{\eta}(x)}{x^3}. \quad (7)$$

The first one $w = w_1$, here called the *unweighted* operator, has been proposed in Refs. [8, 9], the second one $w = w_2$ in Ref. [13] (but for the operator with energy diffusion included), and $w = w_3$ in Refs. [16, 17]. The last one, here called the Kovrizhnikh-Connor operator, has been used in Ref. [12] for Monte Carlo simulations of the bootstrap current.

Simplified collision operators with energy diffusion included

Again, the integrated parallel momentum source strength is estimated from the ‘‘error’’ in the like-particle collision operator of eq. (3) now with C_v^α included leading to

$$\int_0^\infty x^3 \mathcal{P}^\alpha dx = 2\nu_0^\alpha \int_0^\infty \eta(x) \mathcal{K}^\alpha dx.$$

and to the ansatz for \mathcal{P}^α with an arbitrary $w(x)$

$$\mathcal{P}^\alpha(x) = 2\nu_0^\alpha x w(x) F_M^\alpha(x) \frac{\int_0^\infty \eta(x) \mathcal{K}^\alpha dx}{\int_0^\infty w(x) x^4 F_M^\alpha(x) dx}. \quad (8)$$

Only $w = w_1$ and $w = w_2$ of eq. (7) are used for the parallel momentum source function in the collision operator with energy diffusion included in this benchmarking. Equivalent to the correct collision operator, \mathcal{K}^α is obtained from the solution of an integro-differential equation. As is the case for all simplified collision operators, a parallel ion flow leads to an additional contribution to \mathcal{K}^e .

C. Parallel momentum transfer from ions to electrons

Whereas the parallel momentum transfer from electrons to ions is negligible, the inverse process is important and can be formulated by the *generalised* Spitzer equation with the 1st-order ion Rosenbuth potentials as the driving force equivalent to eq. (1),

$$C_{l=1}^\alpha(K_2^e) - \frac{f_t^{\text{eff}}}{f_c^{\text{eff}}} \nu^e K_2^e = -\nu_0^e e^{-x^2} I^{ei}(K^i). \quad (9)$$

Here, $K^i(x_i)$ is the solution of the ion *generalised* Spitzer equation related to the ion parallel flow (e.g. the ion bootstrap current), which drives an additional $K_2^e(x)$ due to the unlike-particle collisions. In principle, this electron flow can be obtained by solving eq. (9). For calculating only the (flux-surface averaged) parallel electron flow, V_{\parallel}^e , the formalism of the adjoint approach [24] is much more convenient.

$$V_{\parallel}^e = v_{th}^e \int_0^{\infty} x^3 K_s^e(x) I^{ei}(K^i) dx$$

where $K_s^e(x)$ is defined by the electron Spitzer equation (with parallel viscosity included)

$$C_{l=1}^e(K_s^e) - \frac{f_t^{\text{eff}}}{f_c^{\text{eff}}} \nu^e K_s^e = -\nu_0^e x e^{-x^2} \quad (10)$$

With integration by parts, the traditional Green's function form is directly obtained

$$V_{\parallel}^e = \frac{4}{\sqrt{\pi}} v_{th}^e \int_0^{\infty} x_i^3 K^i(x_i) G_s^e(x) dx_i$$

with the Green's function (where m_e/m_i -terms are neglected)

$$G_s^e(x) = \frac{3}{2} \left(1 + \frac{6}{5} x^2\right) \int_x^{\infty} K_s^e(x') dx' - \frac{3}{x^3} \int_0^x x'^3 \left(1 - \frac{3}{5} x'^2\right) K_s^e(x') dx'.$$

In the collisional limit, $G_s^e(x)$ agrees well with Hirshman's fit formula [25]. Even for high energy neutral beam injection (NBI), the fast beam particle velocity is typically small compared to v_{th}^e . In the *low-speed-limit* for $x \ll 1$, $G_s^e(0)$ is used for estimating the electron shielding current (Ohkawa current) in the ITER benchmarking [26] of neutral beam current drive. In this approximation, the ion parallel flow, V_{\parallel}^i , drives the electron flow

$$V_{\parallel}^e = G_s^e(0) V_{\parallel}^i \quad \text{with} \quad G_s^e(0) = \frac{3}{2} \int_0^{\infty} K_s^e(x) dx. \quad (11)$$

The electron bootstrap current contribution in Sec. III B driven by the parallel ion flow is calculated from eq. (11) with the corresponding simplified collision operators with momentum source correction in eq. (10) for $K_s^e(x)$.

III. BENCHMARKING RESULTS

Here, the simplified collision operators with momentum source correction are compared with the correct operator with the 1st-order Rosenbluth potentials included. The mono-energetic transport coefficients D_{33} (parallel conductivity) and D_{31} (bootstrap current) are interpolated from a precalculated database of the W7-X “standard” configuration (vacuum) at half the plasma radius. (The benchmarking of the momentum correction technique using the correct linearised collision operator also for tokamaks has been shown in Ref. [6].) Since the simplified collision operators cannot be applied to scenarios with multiple ion species, only a pure electron-proton plasma is assumed in this benchmarking of the parallel conductivity (Sec. III A) and the bootstrap current (Sec. III B).

A. Parallel conductivity

For evaluating the parallel conductivity, the ions are assumed at rest, i.e. $\mathcal{K}_1^i = \Gamma_{33}^i = 0$, and the electron *generalised* Spitzer eq. (1) for parallel momentum correction becomes identical to eq. (10) with the slightly modified definition

$$\mathcal{K}_1^e = \Gamma_{33}^e = f_c^{\text{eff}}(x) \frac{x^4}{1 + \widehat{\eta}(x)} e^{-x^2} = \frac{3\nu_0^e}{(v_{th}^e)^2} \frac{D_{33}^e(x)}{x\langle b^2 \rangle} e^{-x^2}$$

where f_c^{eff} is defined in eq. (2) and the parallel thermodynamic force, A_3^e , is omitted. In Fig. 1, the *generalised* electron Spitzer functions, $S^e(x)$ (on the right), defined by $K_s^e(x) = S^e(x) \cdot \exp(-x^2)$ are compared. Reasonable agreement of both simplified collision operators with energy diffusion included with the weighting functions $w(x) = w_1$ and $w_2(x)$ as well as of the (pure pitch-angle) Kovrizhnikh-Connor operator with the correct one is obtained. Both the strict mono-energetic one and the pure pitch-angle operator with $w(x) = w_1$ lead to a fairly strong deviation, the pure pitch-angle operator with $w(x) = w_2(x)$ is slightly better (the results for these three model operators are not shown in this paper). At higher velocity ($x \geq 3$), the $S^e(x)$ by using the weighted operator with energy diffusion of eq. (8) is very close to the correct result whereas a significant overestimate is found for both of the other simplified operators; see Fig. 1 (on the right). These deviations at higher x can be important for estimating the electron cyclotron current drive efficiency [27] with the adjoint approach. In addition, the collisional [25] and the collisionless [28] limits are well reproduced by the correct operator for very small and very high temperature, respectively.

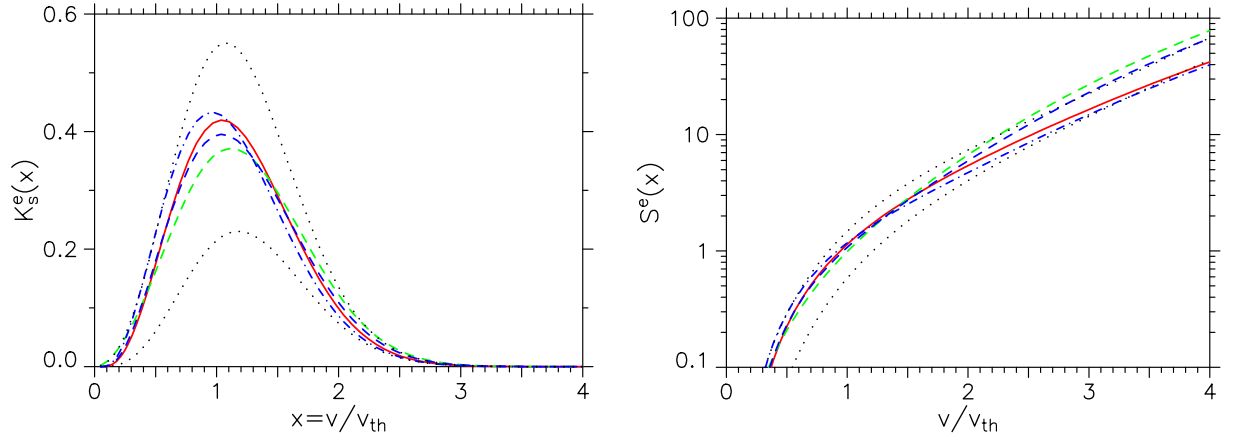


FIG. 1: The functions K_s^e (on the left) and S^e (on the right) vs x for the four collision operators: the correct operator (solid red/black line), the Kovrizhnikh-Connor operator (green/grey dashed line), and the simplified unweighted (blue/black dashed line) and weighted (blue/black dot-dashed line) operators with energy diffusion for $n_e = 10^{20} \text{ m}^{-3}$ and $T_e = 1 \text{ keV}$. The collisional Spitzer function (upper dotted curve) and the collisionless one (lower dotted curve) are given for reference. (Color online)

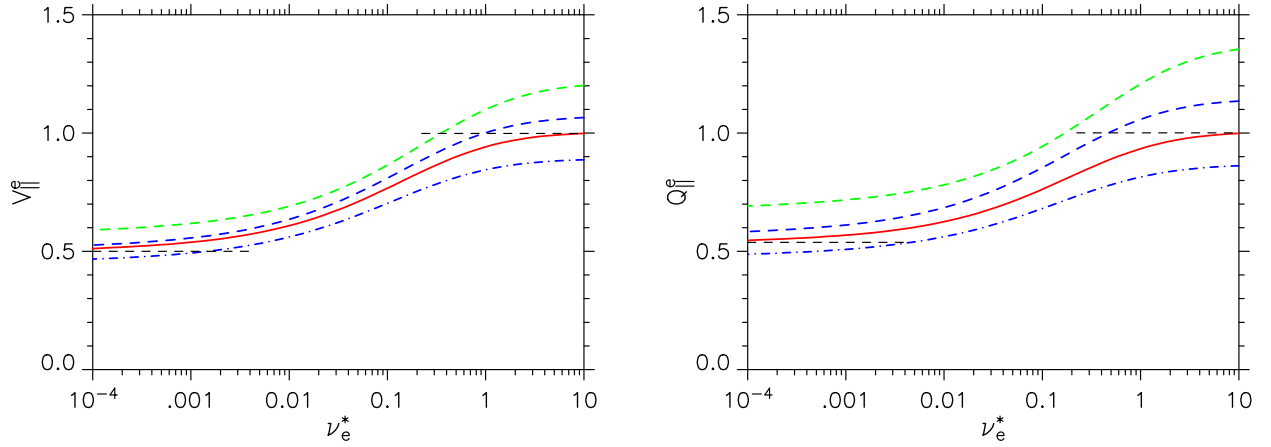


FIG. 2: Moments of the Spitzer functions for the four collision operators vs. the electron collisionality, ν_e^* ; see Fig. 1 for the different operators: the parallel particle flow (on the left) and the parallel energy flow (on the right) both normalised to the collisional limit. The collisional and the collisionless limits (dashed lines) are given for reference. (Color online)

The collision operators are compared with respect to the parallel particle, V_{\parallel}^e , and energy, Q_{\parallel}^e ,

flows in Fig. 2. These flows are defined by

$$V_{\parallel}^e = \int_0^{\infty} x^3 K_s^e(x) dx \quad \text{and} \quad Q_{\parallel}^e = \int_0^{\infty} x^5 K_s^e(x) dx.$$

As was already indicated from Fig. 1, the Kovrizhnikh-Connor operator somewhat overestimates both flows, whereas again reasonable agreement is obtained for both simplified operators with energy diffusion included. The deviations from the correct solution increase with collisionality, where the parallel viscous damping becomes small. The strict mono-energetic operator and the pure pitch-angle collision operators with $w(x) = w_1$ and $w_2(x)$ significantly overestimate both flows.

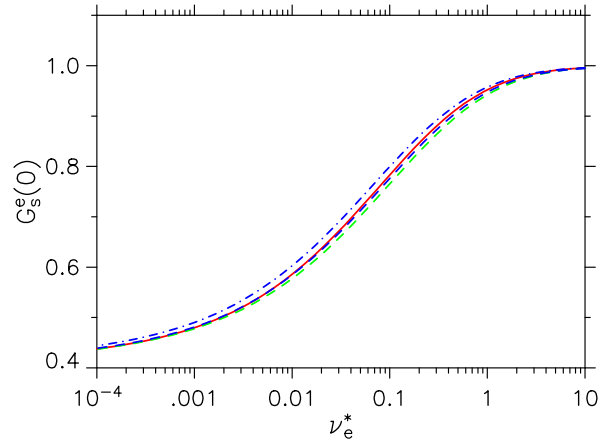


FIG. 3: $G_s^e(0)$ in eq. (11) for the four collision operators vs. the electron collisionality, ν_e^* ; see Fig. 1 for the different operators. (Color online)

Finally, the electron Green's function in the *low-speed-limit*, $G_s^e(0)$, which weights the parallel electron flow driven by its ion counterpart, is compared for the collision operators under investigation. Here, the overall agreement is much better since $G_s^e(0)$ represents simply a normalisation integral of $K_s^e(x)$ with respect to x ; compare eq. (11). Again, a stronger deviation is found for the strict mono-energetic model operator and the unweighted pure pitch-angle one (the weighted operator with $C_v = 0$ and $w = w_2$ is in between).

B. Bootstrap current

The thermodynamic forces driving the bootstrap current are related to the density gradient, n' , the ambipolar radial electric field, E_r , and the temperature gradients, T_e' and T_i' . With the mono-

energetic bootstrap current coefficient, $D_{31}^\alpha(x)$, the flows $\mathcal{K}_1^\alpha = \Gamma_{31}^\alpha$ are defined in Sec. II A. Then, the bootstrap current densities with momentum correction included are defined by

$$j_b^\alpha = q_\alpha v_{th}^\alpha \frac{4}{\sqrt{\pi}} \int_0^\infty \mathcal{K}^\alpha(x) x^3 dx$$

with \mathcal{K}^α from eq. (1). Without momentum correction, the bootstrap current densities are given by

$$q_\alpha v_{th}^\alpha \frac{4}{\sqrt{\pi}} \int_0^\infty \mathcal{K}_1^\alpha(x) x^3 dx = -q_\alpha n_\alpha \frac{4}{\sqrt{\pi}} \int_0^\infty D_{31}^\alpha (A_1^\alpha + x^2 A_2^\alpha) e^{-x^2} x^2 dx.$$

In the figures of this section, all bootstrap current densities are normalised to the collisionless limit without momentum correction for a circular tokamak (in the large aspect ratio limit) for which the bootstrap current coefficient is given by $D_{31}^\alpha = f_t v^2 / (3\epsilon_t t \omega_c^\alpha)$ where $\epsilon_t = r/R$ is the inverse aspect ratio and ω_c^α the cyclotron frequency. With this D_{31}^α , the reference bootstrap current density can be expressed

$$j_b^{\text{ref}} = - \sum_{\alpha=i,e} q_\alpha n_\alpha T_\alpha \frac{f_t}{\epsilon_t t B_0} \left(\frac{(n_\alpha T_\alpha)'}{n_\alpha T_\alpha} - \frac{q_\alpha E_r}{T_\alpha} \right),$$

with the trapped particle fraction $f_t \simeq 1.46\sqrt{\epsilon_t}$ for very small ϵ_t , and the rotational transform, t .

For sufficiently large A_2^α , \mathcal{K}_1^α can change sign with x . Consequently, the two scenarios of a pure density and a pure temperature gradient are analysed here. Furthermore, it was shown in Ref. [6], that the impact of the parallel flows and, consequently, of the parallel momentum conservation on the radial fluxes is negligible for stellarators (except for high collisionalities). Here, the E_r is calculated from the ambipolarity condition of the particle fluxes without momentum correction.

For the correct collision operator defined in eqs. (3-5), the coupled system of integro-differential equations for ions and electrons is solved directly, the momentum exchange between ions and electrons is included here. The parallel momentum source corrections (only for the like-particle collision operators) of eqs. (6) and (8) are restricted to the species α in eq. (1), i.e. two independent integro-differential equations are solved for the simplified operators with energy diffusion (the independent analytical solutions for the pure pitch-angle collision operators are given in eq. (6)). For all the simplified operators, the momentum exchange from ions to electrons described by eq. (11) results in a flux-surface-averaged electron flow which is added to the one driven by the radial gradients (the momentum transfer from electrons to ions is neglected).

An important optimisation criterium in the W7-X stellarator concept was a minimisation of the bootstrap current to allow for the control of the edge rotational transform and for a proper island

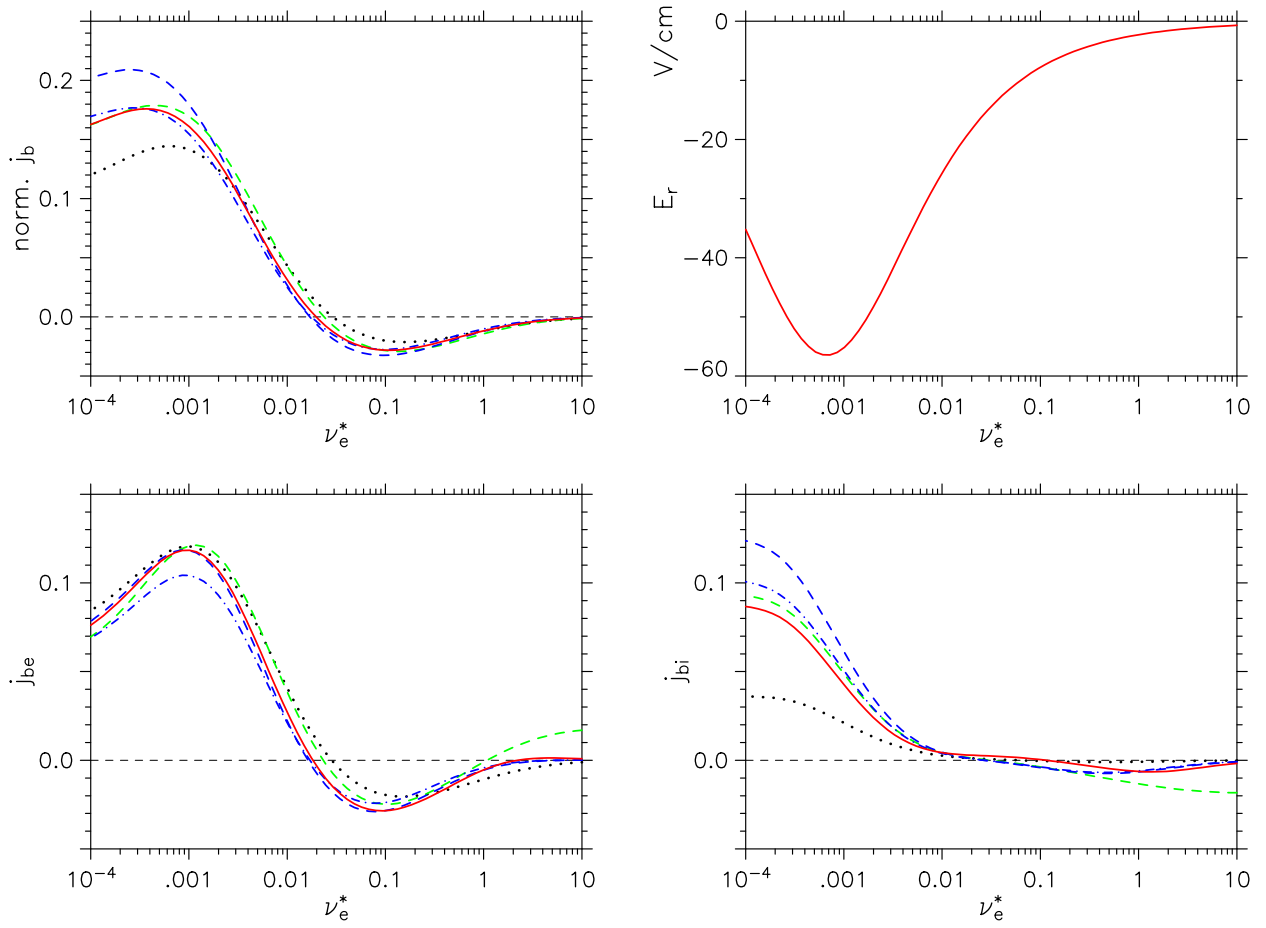


FIG. 4: Bootstrap current for a pure density gradient vs. collisionality, ν_e^* : $n'/n = -1 \text{ m}^{-1}$, $n = 10^{20} \text{ m}^{-3}$, $T_e = T_i$, $T'_e = T'_i = 0$; see Fig. 1 for the different operators. Norm. ion bootstrap current (lower right plot), electron one (lower left), total current (upper left), and ambipolar radial electric field (upper right plot). Flows without momentum corrections (dotted lines) are given for reference. (Color online)

divertor operation [29]. This is most successfully realised in the high-mirror W7-X configuration [6] where the bootstrap current can even change sign by increasing the toroidal field ripple [30]. For the standard W7-X configuration, however, the bootstrap current increases the edge rotational transform and can have a significant effect on the magnetic island topology in the divertor. On the other hand, this configuration is characterised by significantly reduced neoclassical transport and will be important for high-performance W7-X operation. Thus, this standard W7-X configuration is selected here for benchmarking of the impact of the different collision operators on the bootstrap current.

The scenarios with a pure density gradient (and the ambipolar E_r) where the momentum cor-

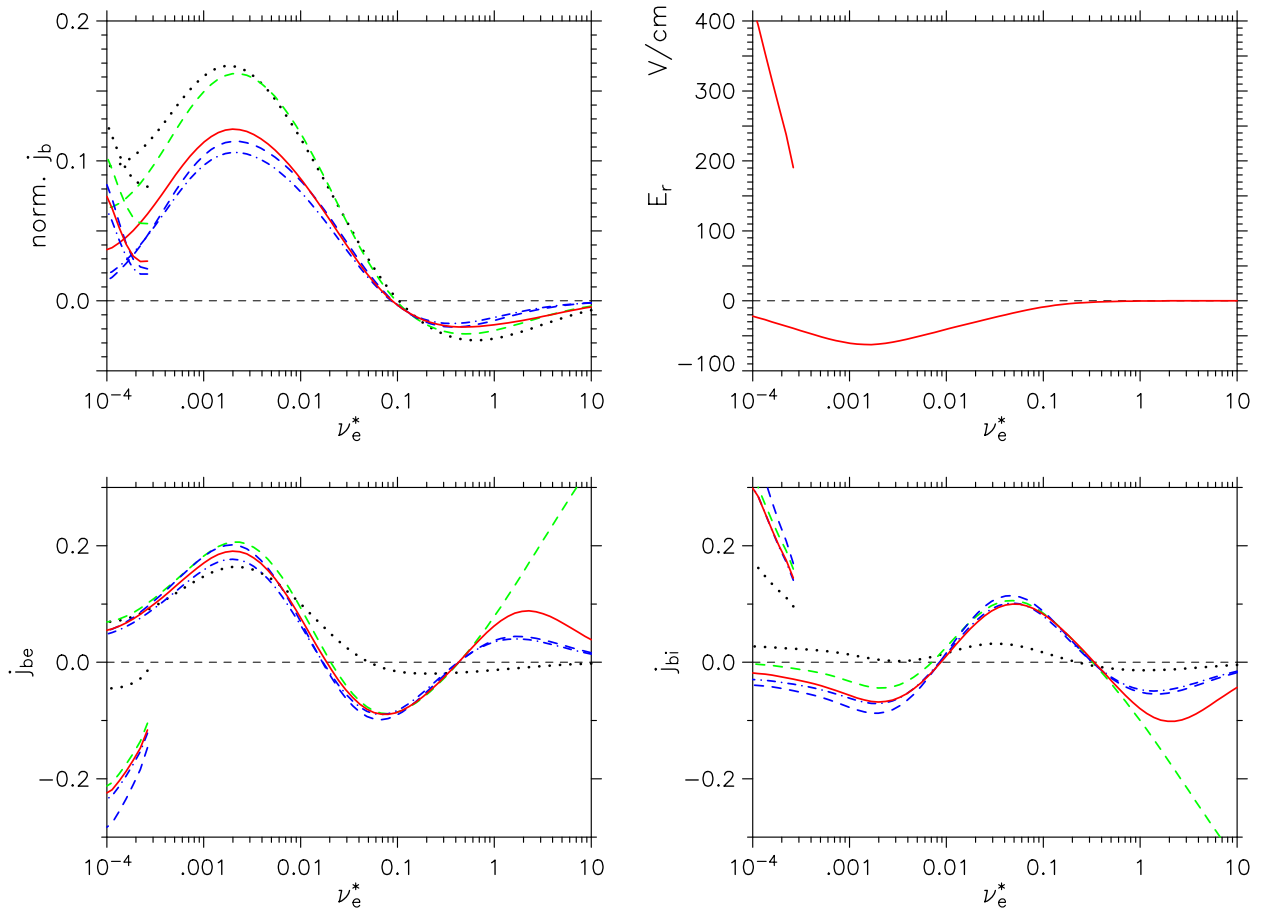


FIG. 5: Bootstrap current for pure temperature gradients vs. collisionality, ν_e^* : $T_e'/T_e = T_i'/T_i = -1 \text{ m}^{-1}$, $n = 10^{20} \text{ m}^{-3}$, $T_e = T_i$, $n' = 0$; compare Fig. 4. (Color online)

rection leads to an increased bootstrap current at low collisionalities and with a pure temperature gradients (again with E_r) with the contrary effect are shown in Figures 4 and 5. For the pure n' scenario, the ion parallel flow is rather small at intermediate and high collisionalities since the ambipolar E_r nearly compensates the n' force (an equivalent simulation with $E_r = 0$ assumed leads also to fairly large ion flows). At high collisionalities in the $n' = 0$ scenario, both simplified collision operators with energy diffusion included underestimate the ion flow whereas the pure pitch-angle operators of eq. (8) significantly overestimate the ion flow; see Fig. 5. Here, the parallel viscous damping is very small, and the approximations in the collision operators become crucial for the total parallel momentum conservation. For the pure n' scenario of Fig. 4, the bootstrap current is increased over the case without momentum correction (dotted line) at low collisionalities, but rather large differences are obtained for the different collision operators: very good agreement with the correct operator is obtained both for the Kovrizhnikh-Connor model and

the one with energy diffusion and $w = w_2$.

For the pure T' scenario of Fig. 5, the impact of momentum correction on both ion and electron flows is fairly large compared to the case without correction. Since for the higher collisionalities the electron flow mainly compensates the ion flow, the deviations in the total bootstrap current are rather small. At low collisionalities, in particular, the impact of momentum correction becomes significant. Here, an additional “electron-root” with strongly positive E_r is found, which by evaluating the thermodynamic principle of Ref. [31] cannot be realised. In this example, both model operators with energy diffusion included show reasonable agreement with the correct one for the bootstrap current whereas all operators of eq. (6) result in a significant overestimate (the strict mono-energetic operator is here not the worst one). In particular, for the model operator with the w_2 -energy weighting in the momentum source function of eq. (8) the best agreement with the correct one is found in all such bootstrap current simulations.

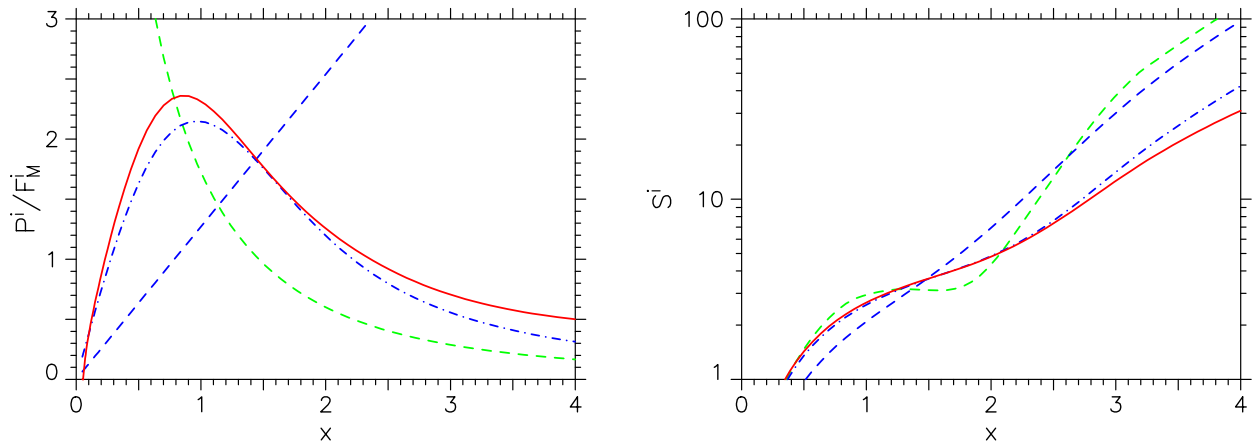


FIG. 6: The parallel momentum source function, \mathcal{P}^i/F_M^i (on the left), and the ion Spitzer function, S^i (on the right), vs. x for the scenario of Fig. 5 at $T_i = 1$ keV ($\nu_e^* = 0.079$) for the collision operators with energy diffusion. (Color online)

Next, the impact of the weighting function, $w(x)$, in eqs. (6) and (8) is analysed in more detail. Figure 6 shows the ion parallel momentum source function, $\mathcal{P}^i(x)$ (with the Maxwellian extracted) as well as the ion Spitzer function, $S^i(x)$ ($\mathcal{K}^i = S^i \cdot \exp(-x^2)$) for the scenario of Fig. 5 at an intermediate collisionality. In the correct collision operator, the small collisional electron-ion interaction in eq. (5) is included equivalent to all examples shown in this Section III B. Whereas the unweighted collision operator with energy diffusion ($w(x) = 1$) leads to significant deviations in particular at $x \geq 2$, the weighted operator (with $w = w_2(x)$) is in fairly good agreement with the

correct solution. This result is also found at other collisionalities. At high collisionalities, however, $\mathcal{P}^i(x)$ has an equivalent shape, but the magnitude is smaller leading to the reduced parallel ion flow in Fig. 5 compared to the correct solution. These findings for the parallel ion flow are rather similar to the electron Spitzer function results shown in Fig. 1. Finally, the Kovrizhnikh-Connor operator with the weighting function $w(x) = \hat{\eta}(x)/x^3$ leads to a very strong momentum source at small x ($w(x) \propto 1/x^2$ for $x \ll 1$) which is not the case for the other simplified model operators. With respect to the ion flow, these discrepancies, in particular at larger x , are strongly reduced in the convolution with the Maxwellian leading to the rather reasonable agreement shown in Fig. 5.

IV. SUMMARY AND CONCLUSIONS

Several linearised collision operators with parallel momentum source corrections are benchmarked against the correct form based on the first-order Rosenbluth potentials for both the parallel conductivity and the bootstrap current. Simplified collision operators of this type are commonly used in δf -Monte Carlo simulations, but a detailed analysis of their reliability for estimating the parallel flows was previously lacking.

Generally, rather reasonable agreement of the simplified operators with the correct formulation is found. The strict mono-energetic collision operator as the most simplified one represents something like a worst case of an operator with momentum conservation. The deviations of this model operator from the correct solution, however, is comparable to the pure pitch-angle collision operator without energy weighting. Except for higher collisionalities, rather reasonable agreement is only found for this type with an energy-weighting function which corresponds to the energy weight of the “error” in the like-particle momentum conservation (i.e. $w(x) = \hat{\eta}(x)/x^3$). This Kovrizhnikh-Connor model operator [16, 17] without energy diffusion, however, leads to a significant overestimate of the momentum correction for the bootstrap current in case of a pure temperature gradient scenario where the driving force changes sign with respect to energy. For this case, the energy diffusion contribution in the model operators becomes important.

The unweighted collision operator with energy diffusion is less accurate compared with the weighted one with $w(x) = \eta(x)/x^3$ (also corresponding to the energy weight of the “error” in the like-particle momentum conservation), for which very good agreement with the correct collision operator was found (even for the corresponding Spitzer functions). This collision operator with the weighted parallel momentum source correction suggested in [13] is thus to be favoured for

calculating the parallel flows.

Acknowledgments

The authors acknowledge helpful discussions with A. Bergmann, M.Yu. Isaev and R. Kleiber, and in particular with P. Helander who pointed out Refs. [13, 19, 20].

-
- [1] M.N. Rosenbluth, W.M. MacDonald, and D.L. Judd, *Phys. Rev.* **107**, 1 (1957).
 - [2] L. Spitzer and R. Härm, *Phys. Rev.* **89**, 977 (1953).
 - [3] M. Taguchi, *Phys. Fluids B* **4**, 3638 (1992).
 - [4] H. Sugama and S. Nishimura, *Phys. Plasmas* **9**, 4637 (2002).
 - [5] H. Sugama and S. Nishimura, *Phys. Plasmas* **15**, 042502 (2008).
 - [6] H. Maaßberg, C.D. Beidler, and Y. Turkin, *Phys. Plasmas* **16**, 072504 (2009).
 - [7] C.D. Beidler, M.Yu. Isaev, S.V. Kasilov, W. Kernbichler, H. Maaßberg, D. S. Murakami, V.V. Némov, M. Schmidt, D.A. Spong, V. Tribaldos, and A. Wakasa, *Proc. 22nd IAEA Fusion Energy Conf.*, Geneve, 2008; www-pub.iaea.org/MTCD/Meetings/fec2008pp.asp_th_p8-10.pdf.
 - [8] P.J. Catto and K.T. Tsang, *Phys. Fluids* **20**, 396 (1977).
 - [9] X.Q. Xu and M.N. Rosenbluth, *Phys. Fluids* **B3**, 627 (1991).
 - [10] A.M. Dimits and B.I. Cohen, *Phys. Review E* **49**, 709 (1994).
 - [11] Z. Lin, W.M. Tang, and W.W. Lee, *Phys. Plasmas* **2**, 2975 (1995).
 - [12] A. Bergmann, E. Strumberger, and A.G. Peeters, *Nucl. Fusion* **45**, 1255 (2005).
 - [13] I.G. Abel *et al.*, *Phys. Plasmas* **15**, 122509 (2008).
 - [14] J.G. Cordey, E.M. Jones, and D.F.H. Start, *Nucl. Fusion* **19**, 249 (1979).
 - [15] D.F.H. Start and J.G. Cordey, *Phys. Fluids* **23**, 1477 (1980).
 - [16] M.N. Rosenbluth, R.D. Hazeltine, and F.L. Hinton, *Phys. Fluids* **15**, 116 (1972).
 - [17] J.W. Connor, R.C. Grimm, R.J. Hastie, and P.M. Keeping, *Nucl. Fusion* **13**, 211 (1973).
 - [18] A. Bergmann, A.G. Peeters, and S.D. Pinches, *Phys. Plasmas* **8**, 5192 (2001).
 - [19] P.J. Catto and D.R. Ernst, *Plasma Phys. Control. Fusion* **51**, 062001 (2009).
 - [20] H. Sugama, T.-H. Watanabe, and M. Nunami, *Phys. Plasmas* **16**, 112503 (2009).
 - [21] G. Grieger, W. Lotz, P. Merkel, J. Nührenberg, J. Sapper, E. Strumberger, H. Wobig, the W7-X Team,

- R. Burhenn, V. Erckmann, U. Gasparino, L. Giannone, H.J. Hartfuss, R. Jaenicke, G. Kühner, H. Ringler, A. Weller, F. Wagner, and the W7-AS Team, *Phys. Fluids B* **4**, 2081 (1992).
- [22] S.P. Hirshman, K.C. Shaing, W.I. van Rij, C.O. Beasley, Jr., and E.C. Crume, *Phys. Fluids* **29**, 2951 (1986).
- [23] W.I. van Rij and S.P. Hirshman, *Phys. Fluids B* **1**, 563 (1989).
- [24] M. Taguchi, *Plasma Phys. Control. Fusion* **31**, 241 (1989).
- [25] S.P. Hirshman, *Phys. Fluids* **23**, 1238 (1980).
- [26] T. Oikawa and *et al.*, *Proc. 22nd IAEA-FEC, Geneva*, IT/P6-5 (2008).
- [27] N.B. Marushchenko, C.D. Beidler, and H. Maaßberg, *Fusion Sci. Techn.* **55**, 180 (2009).
- [28] M. Romé, V. Erckmann, U. Gasparino, and N. Karulin, *Plasma Phys. Control. Fusion* **40**, 511 (1998).
- [29] D. Sharma, Y. Feng, and F. Sardei, *Nucl. Fusion* **46**, S127 (2006).
- [30] J. Geiger, H. Maaßberg, and C.D. Beidler, *35th EPS Plasma Physics Conference, Hersonissos, Crete*, http://epsppd.epfl.ch/Hersonissos/pdf/P2_062.pdf (2008).
- [31] H. Maaßberg, C.D. Beidler, U. Gasparino, M. Romé, the W7-AS Team, K.S. Dyabilin, N.B. Marushchenko, and S. Murakami, *Phys. Plasmas* **7**, 295 (2000).